THE JOURNAL OF PHYSICAL CHEMISTRY B

Article

pubs.acs.org/JPCB

Pressure-Induced Changes in the Fluorescence Behavior of Red Fluorescent Proteins

Eric A. Pozzi, Linda R. Schwall, Ralph Jimenez, and J. Mathias Weber*

JILA, NIST and Department of Chemistry and Biochemistry, University of Colorado, Boulder, Colorado 80309-0440, United States

ABSTRACT: We present an experimental study on the fluorescence behavior of the red fluorescent proteins TagRFP-S, TagRFP-T, mCherry, mOrange2, mStrawberry, and mKO as a function of pressure up to several GPa. TagRFP-S, TagRFP-T, mOrange2, and mStrawberry show an initial increase in fluorescence intensity upon application of pressure above ambient conditions. At higher pressures, the fluorescence intensity decreases dramatically for all proteins under study, probably due to denaturing of the proteins. Small blue shifts in the fluorescence spectra with increasing pressure were seen in all proteins under study, hinting at increased rigidity of the chromophore environment. In addition, mOrange2 and mStrawberry exhibit strong and abrupt changes in their fluorescence spectra at certain pressures. These changes are likely due to structural modifications of the hydrogen bonding environment of the chromophore. The strong differences in behavior between proteins with identical or very similar chromophores highlight how the chromophore environment contributes to pressure-induced behavior of the fluorescence performance.

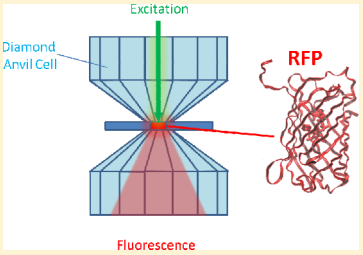

INTRODUCTION

Green Fluorescent Protein (GFP) derived from *Aequorea victoria* and its variants from *Discosoma striata, Entacmaea quadricolor* and others are widely used as noninvasive biomarkers for studying biochemical processes *in vivo*.[1,2] These fluorescent proteins (FPs) have a structure with 11 β-sheets forming a barrel around a central chromophore.[1]

By genetically engineering chromophores and their immediate surroundings, emission wavelengths spanning nearly the entire visible spectrum have been created.[2−5] While GFP has probably been the most widely studied FP, Red Fluorescent Proteins (RFPs) have received much attention in recent years because their fluorescence can be easily distinguished from the yellow-green autofluorescence of cells and because the reduced light scattering of longer wavelength photons permits their use as biomarkers in thick tissues.[3]

In GFP, the chromophore autocatalytically matures from amino acid residues in the presence of molecular oxygen by internal tripeptide cyclization, dehydration and oxidation.[1] In cyan- and green-emitting FPs, chromophores are usually chemically identical to that of GFP.[6,7] In contrast, the chromophores of the RFPs go through a multistep reaction that involves covalent modification of the protein backbone to create a red-shifted variant by extending the conjugated system of the chromophore into the peptide backbone through an acylimine linkage.[4,8,9] This chemical diversity of chromophores makes the RFPs an interesting target for investigating their reactions to physical stimuli. Among the variants studied in the present work, mKO and mOrange2 contain tricyclic chromophores, while mCherry, TagRFP-S, TagRFP-T and mStawberry contain bicyclic chromophores (see Figure 1). The additional ring in the variants mKO and mOrange2 is a substituted dihydrothiazole ring in mKO and a substituted dihydrooxazole ring in mOrange2.[8] In contrast, this ring is absent in mCherry, TagRFP-S, TagRFP-T and mStrawberry.[4,10] The stereochemistry of the double bond between the

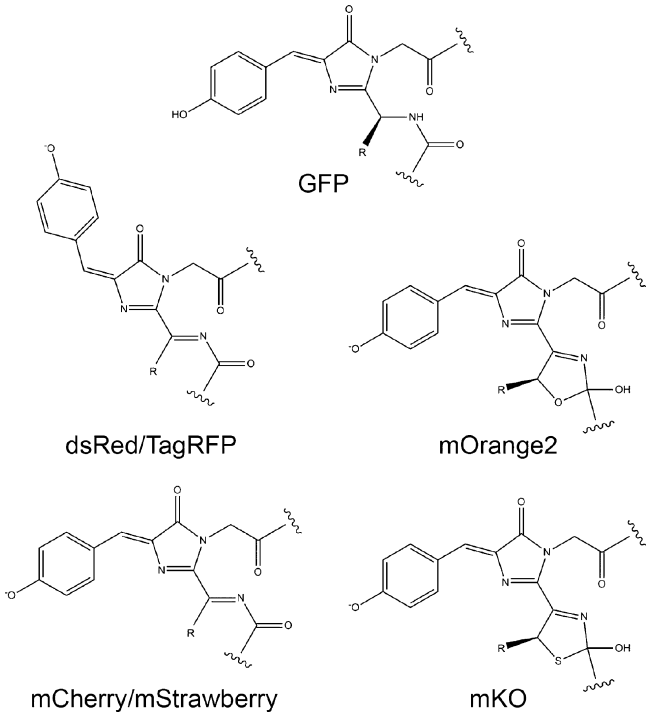

Figure 1. Simplified chromophore structures of FPs investigated here and of GFP.

Received: June 20, 2012
Revised: August 3, 2012
Published: August 3, 2012

imidazolinone ring and the hydroxyphenyl ring allows for further discrimination between the chromophores. In the mFruit proteins studied here, this double bond is in the *cis* conformation, but the same double bond is in the *trans* conformation in TagRFP-S and TagRFP-T.[10]

GFP and its variants are highly resistant to denaturing by temperature and pH, which can be attributed to the β-barrel tertiary structure.[11] Different from the influence of temperature, pH and denaturing agents, which have multiple effects on a system (total energy, volume, covalent bonds), perturbation of a protein by hydrostatic pressure only changes inter- and intramolecular distances[12] in the pressure range of up to ca. 1 GPa (above which neat water solidifies[13]). These changes can lead to conformational modifications and ultimately to denaturing. The stability of FPs with respect to pressure can provide useful information about their properties.[11,14] For example, fluorescence measurements at various pressures can provide insight into perturbations to the hydrogen bonding network around the chromophore and how changes in chromophore mobility affect the fluorescence intensity of a FP.

The effects of hydrostatic pressure on green,[11,14−17] blue[16,18−20] and yellow variants,[21,22] as well as dsRed[16] (the only RFP studied so far at high pressures) have been previously studied and show a variety of behavior. A number of GFP-based mutants were found to retain or even slightly increase (by ca. 20%) their ambient fluorescence intensities by increasing pressure up to 600 MPa.[14,16] Scheyhing et al. observed wild-type GFP to retain its secondary structure up to 1.3 GPa using infrared absorption spectroscopy.[11] BFP was found to exhibit an increase in fluorescence intensity by a factor of 1.8 upon an increase in pressure up to ca. 500 MPa.[19] In contrast, upon increase of pressure to 50 MPa, the fluorescence intensity of citrine, a yellow emitting FP, was observed to increase, after which a drastic decrease in intensity and a concomitant blue shift were found.[21,22] With the exception of dsRed, which exhibits a small increase in fluorescence intensity at low pressures (up to 200 MPa),[16] the effects of pressure on RFPs with their different chromophore variants have not been studied so far.

In this paper, we present data on the fluorescence intensities and emission spectra of the RFPs mKO, mOrange2, TagRFP-S, TagRFP-T, mCherry and mStrawberry as a function of pressure up to several GPa. An accompanying paper by Laurent et al.[23] describes molecular dynamics (MD) and QM/MM (quantum mechanics-molecular mechanics) simulations performed on mStrawberry and mCherry that shed light on the molecular origins of the observed pressure induced changes in fluorescence behavior.

METHODS

Sample Preparation. Fluorescent proteins were purified from cultures of Top10 *E. coli* cells transformed with the appropriate pBAD-based vectors for each protein. Cells were harvested 16−20 h after induction with 0.2% arabinose. The pellets were chemically lysed with added EDTA-free Protease Inhibitor, centrifuged and 0.45-μm-filtered. The 6X-His-tagged proteins were purified via Ni/NTA chromatography, then buffer-exchanged into 50 mM Tris, 50 mM NaCl pH 7.5 buffer.

High Pressure Generation. Blank high pressure gaskets (type 302 stainless steel, initial thickness 250 μm) were preindented to a final thickness of 90−100 μm in a gas-membrane driven diamond anvil cell (type Ia 16-sided diamond anvils, base diameter 2.5 mm, culet 0.50 mm, NA = 0.54). The sample volume was created in each gasket by laser drilling a hole with ca. 150 μm diameter in the center of each preindented gasket. Samples (15−30 μMol protein concentration) were loaded into the diamond anvil cell (DAC) together with ruby grains for pressure measurement. Pressures were determined by evaluating the R_1 ruby fluorescence wavelength upon irradiation with radiation from a red laser diode (λ = 635 nm, ca. 0.2 W/cm^2). Cell pressure variation by variation of the gas-membrane pressure was followed by 30−45 min equilibration periods. Typically, no change in the peak wavelength of the R_1 line was observed 20 min after pressure increase in the gas-membrane. The peak position of the R_1 line for each data point was determined by a Gaussian fit of the R_1 line in the ruby fluorescence spectrum. The pressure inside the DAC was then calculated using the measured peak wavelength λ of the R_1 line in equation:[24]

$$p = \frac{1904}{7.665}\left[\left(\frac{\lambda}{\lambda_0}\right)^{7.665} - 1\right] \quad (1)$$

where λ_0 is the peak wavelength at ambient pressure. The error of the pressure measurement is due to the finite pixel resolution and the error in the calibration equation. The pixel resolution results in error bars of ±75 MPa (see below for more information on the spectrometer used). The ruby calibration equation was reported to have a maximum error of ±3%,[24] becoming the most relevant contribution above 2.5 GPa. The sample was monitored with a microscope during pressurization to ensure that the sample compartment did not shift or deform significantly by plastic deformation of the gasket. Pressure runs were performed starting at low pressures and pressure was increased in steps of 100−200 MPa. The lowest pressures achieved were usually slightly (ca. 100 MPa) higher than ambient pressure due to pressure applied during closing and sealing of the DAC. Pressure runs were performed several times for each protein on different days. All reported pressure runs were performed by monotonically increasing the pressure to the final pressure of the run and discarding the sample.

Fluorescence Spectroscopy. Samples were excited by irradiation with light from a diode-pumped frequency-doubled Nd:YAG laser (λ = 532 nm, ca. 0.05 W/cm^2). Samples were irradiated with green light for up to 20 s. at each pressure. Fluorescence was collected using a matched achromatic pair (focal lengths f_1 = 30 mm and f_2 = 100 mm) and the laser excitation line was filtered using a long pass filter (cutoff at 550 nm). The fluorescence light was focused into a multimode fiber (400 μm diameter) and fed into a fiber-optic spectrometer. The ruby fluorescence was analyzed using a fiber-optic spectrometer (grating with 1800 lines/mm, slit width 10 μm, 2048 pixel CCD detector array, 0.07 nm resolution). The protein fluorescence was analyzed with a broadband fiber-optic spectrometer (grating with 300 lines/mm, slit width 50 μm, 2048 pixel CCD detector array, 2.4 nm resolution). Spectra were acquired for up to 200 ms integration time per spectrum and up to 100 spectra were averaged at each pressure. Test measurements using continuous irradiation with the 635 nm pressure probe wavelength and the 532 nm green excitation laser revealed only small changes (<10%) in fluorescence intensity within 10 min except for mOrange2 (ca. 25% photobleaching after 10 min) and mCherry (ca. 12% increase of fluorescence intensity after 10 min). For the short accumulated irradiation times in the pressure dependent runs, we assume that effects of kindling or photobleaching are

negligible. Test experiments using excitation with 488 nm showed the same fluorescence behavior as with 532 nm.

Data Analysis. Integrated fluorescence intensities as a function of pressure were extracted from each run and normalized to 1 in their maxima. The integration intervals were 550−630 nm for TAG-RFP-S, TAG-RFP-T and mOrange2, 570−650 nm for mCherry, 550−650 nm for mStrawberry and 544−650 nm for mKO. Multiple fluorescence intensity curves as a function of pressure were linearly interpolated to create a grid of 100 MPa steps and then averaged. In principle, a measure of the uncertainty associated with these averaged curves can be determined by calculating the differences between intensities of each interpolated data set and the averaged interpolated data set for each pressure. The standard deviation of these differences can be used as an estimate for the error in the fluorescence intensity versus pressure curve on the normalized intensity scale. The error for TagRFP-T was calculated to be 0.14, whereas the other five studied RFPs were calculated to have errors no greater than 0.07. We note that this method could introduce a bias, since test measurements suggest that the intensities can be dependent on the way in which pressure is applied. The direction and the rate of pressure change may influence the measured intensities to a small extent. In order to illustrate the behavior in different pressure runs, integrated intensities are reported by averaged curves as described above, together with the data points normalized integrated intensities for all pressure runs.

RESULTS AND DISCUSSION

Figure 2 shows the fluorescence intensities of the proteins under study as a function of hydrostatic pressure up to 2 GPa. Of the six RFPs we studied, two (mKO and mCherry) exhibit a continuous decrease in fluorescence intensity upon pressure increase. The four other RFPs show a peak in their fluorescence intensities at intermediate pressures, followed by a decrease at high pressure. The modifications in fluorescence intensities are large over the observed pressure region for all species studied. At the highest pressures, all RFPs lose more than 80% of their maximum fluorescence intensity. Above 1 GPa, however, water solidifies, so the change in fluorescence may be accompanied by a phase change of the buffer, and we caution that this will severely affect protein behavior.

Increases in fluorescence intensity for mOrange2 and TagRFP-S at intermediate pressures (up to ca. 500 MPa) are comparable to the pressure behavior of other FPs.[14,16,19,25] Interestingly, the fluorescence intensity of mStrawberry and TagRFP-T increased by factors of ca. 2 in this intermediate pressure regime. This pressure-induced increase is among the highest reported to date, similar to the case of BFP, whose fluorescence intensity increased by a factor of 1.8 upon pressurization to ca. 500 MPa.[19] An increase in fluorescence intensity can be rooted in changes of different factors. The brightness of a FP is defined as the product of its absorption coefficient and its fluorescence quantum yield, therefore an increase in brightness can be caused by an increase of either property.

An increase in quantum yield could be the result of increased rigidity upon pressurization, which will restrict the volume accessible for conformational changes and structural fluctuations in the chromophore pocket, similar to the temperature dependent changes observed in BFP.[19] Such a restriction of motion could suppress radiationless transitions coupled to

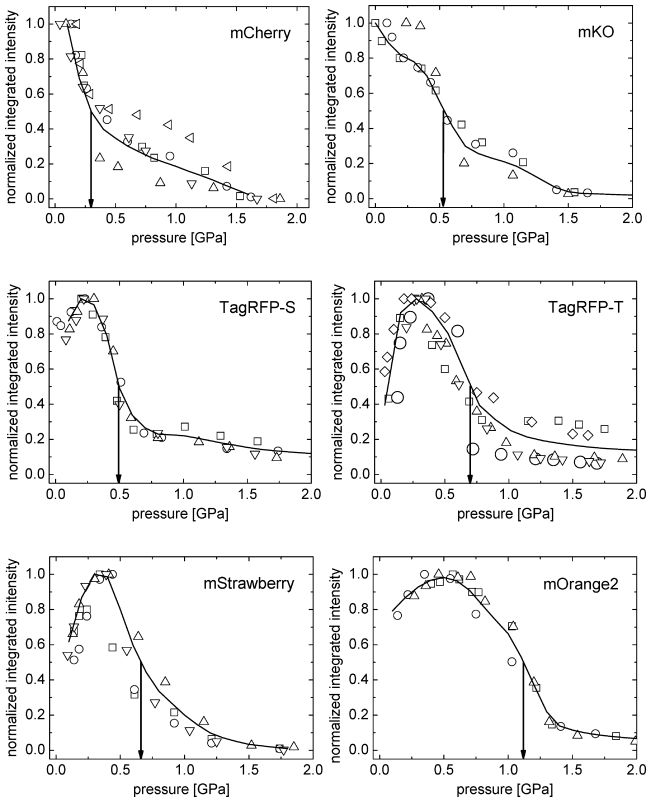

Figure 2. Pressure-dependent fluorescence intensity curves of mCherry (top left), mKO (top right), TagRFP-S (center left), TagRFP-T (center right), mStrawberry (bottom left) and mOrange2 (bottom right). Arrows denote the pressures at which the fluorescence intensity of each variant has decreased to half of its maximum value ($p_{1/2}$, see also Table 1). Different symbols correspond to different pressure runs, the full lines are averaged curves, renormalized to 1 at their respective maximum values.

thermal motion. The compressibility of a protein is typically of the order of 0.3−1.5 × 10^{-4} MPa^{-1},[19,26−28] and the β-barrel proteins are likely to have compressibilities on the lower end of this range.[26] A pressure increase of 1 GPa therefore results in a volume reduction of ca. 5% of the protein. This loss of volume translates into a reduced mobility of the chromophore. Molecular dynamics simulations by Mauring and co-workers[26] found decreasing root-mean-square deviations (rmsd) in BFP at elevated pressures, although they did not specifically connect this observation with the increased fluorescence intensity observed experimentally.[19] More to the point, Goedhart et al. recently used a structure guided evolution approach to improve the brightness of a cyan FP, citing rigidity as a key element for optimized quantum yield.[29] rmsd distributions contain information on structural changes and thermal motion (encoded in the rmsd magnitude) as well as the range of thermal motion (encoded in the width of the rmsd distribution). Laurent et al.[23] performed 50 ns MD simulations on mCherry and mStrawberry, described in a companion paper to the present work. They report reduced rmsd as well as narrower rmsd distributions for intermediate pressures indicating a reduced range of structural fluctuations and thermal motion. At higher pressures (above 600 MPa), the backbone rmsd increases again for both proteins. Laurent et al.[23] show that thermal fluctuations in mStrawberry and mCherry indeed decrease for intermediate pressures, typically in the range where increase of fluorescence intensity is

dx.doi.org/10.1021/jp306093h | J. Phys. Chem. B 2012, 116, 10311−10316

observed, before increasing again. Interestingly, their MD simulations suggest that—on the ns time scale—mStrawberry is more mobile than mCherry, and the suppression of thermal motion is more pronounced for mStrawberry than for mCherry. As a result, the number of water molecules in the vicinity of the chromophore decreases substantially at intermediate pressures for mStrawberry, while these changes are calculated to be much smaller in mCherry. Differences in rigidity and in the number of internal water molecules could explain the strong difference in fluorescence intensity behavior between the two variants. In addition, the MD results indicate that thermal fluctuations in the barrel are more pronounced than for the chromophore, highlighting the role of the barrel for the difference in protein stability.

Structural change is connected with a reaction volume change. Verkhusha et al.[16] used a phenomenological analysis of fluorescence intensities of FPs assuming a two-state model of protein conformational change to obtain this volume change (among other parameters) associated with the pressure behavior. We note that the pressure range investigated in ref.[16] was much smaller than in the present work. As a result, the fluorescence behavior observed in our data likely spans more than a single conformational change and cannot be straightforwardly described by a two-state model beyond ca. 500 MPa. In addition, we evaluated data for only those variants where the initial pressure changes are not too abrupt and a sufficient number of data points are available during the first change. With these limitations in mind, we have obtained volume changes for the transitions between the native form and the first conformational change in mKO, mOrange2, mCherry and mStrawberry to be (−10 ± 3) mL/mol, (−16 ± 1) mL/mol, (−6.8 ± 0.9) mL/mol and (−52 ± 13) mL/mol, respectively. These changes in reaction volume are somewhat smaller in magnitude, but overall similar to those reported by Verkhusha et al.[16] for several different FPs. The volume change for mCherry is smaller than that for mStrawberry, which is qualitatively consistent with the MD result[23] that mCherry is more rigid than mStrawberry.

On the basis of the known quantum yields of the proteins under study (see Table 1), it is possible that some of the increase in fluorescence intensity can be attributed to an increase in absorption cross section in addition to an increase in quantum yield. Unfortunately, our setup does not allow direct measurement of the absorption cross section to clarify this issue at present. There are no calculations on pressure induced changes in TagRFP-T absorption. In the case of mStrawberry and mCherry, Laurent et al.[23] calculate a modest increase (ca. 4% at 300 MPa, followed by ca. 6% decrease at 900 MPa) in oscillator strengths, suggesting that the larger share of pressure-induced fluorescence increase is due to increased quantum yield.

We note that at high excitation laser intensities, enhancement of the *apparent* absorption coefficient of a chromophore could in principle be caused by a decrease of the time the chromophore spends in dark states that are assumed to play a role in photochemical processes of RFPs.[30,31] However, under our experimental conditions, ground state recovery times would need to be of the order of ms to play a role here, which is approximately 10^3-fold longer than the estimated[30] and measured ground state recovery times for these and other proteins.

All six RFPs eventually lose fluorescence intensity as pressure is increased. The simplest explanation for this observation is that the proteins can be expected to denature or undergo strong chromophore pocket deformation at high pressures.[32,33] High pressure changes H-bonded networks and pressure-induced denaturing is thought to involve forcing water molecules into the hydrophobic regions of the molecule, disrupting its structure.[33] The retention of some residual fluorescence intensity without much change in the fluorescence spectrum (except mOrange2 and mStrawberry, see below) and the rather large pressure range through which fluorescence is lost in most of the studied RFPs suggest that most chromophores do not undergo covalent modifications, but that increased probability for radiationless de-excitation or conformational change gradually lead to loss of fluorescence. The pressures $p_{1/2}$ at which fluorescence intensity decreases to half of its maximum value can serve as a measure of stability for the chromophore environment. Using this figure of merit, mCherry seems to have the most fragile pocket, while mOrange2 has the most robust chromophore pocket of the RFPs tested (see Table 1). Using the ambient (I_0) and maximum (I_{max}) fluorescence intensities, the value $I_{max}/(I_0 \cdot p_{1/2})$ can be used as a measure of pressure-induced variability of fluorescence intensity, showing mOrange2 as having the lowest variability and TagRFP-T having the highest.

Our observations of the pressure-dependent fluorescence intensities are complemented by measurements of the pressure-dependent fluorescence spectra shown in Figure 3. All RFPs studied here exhibit small blue shifts with increasing pressure and some show small shifts back toward longer wavelengths at the highest pressures. In mStrawberry and mOrange2, these weak shifts are superimposed on stronger changes in the fluorescence spectra that will be discussed further below. The weak blue shifts observed with increasing pressure in most of the fluorescence spectra are consistent with a pressure-induced increase in rigidity, as calculated by Laurent et al.[23] This lends further credibility to the idea that structural changes in the excited state are considerably hindered at elevated pressures, leading to less sampling of dark excited states and possibly a lower probability for radiationless transitions, resulting in higher quantum yields.[18]

A very interesting observation is that mStrawberry and mOrange2 undergo abrupt and drastic changes in their fluorescence spectra upon pressurization (see Figure 3). The peak of the fluorescence emission spectrum in mStrawberry shifts by ca. 800 cm^{-1} from 596 to 568 nm at pressures around

Table 1. Properties of RFPs Studied in This Paper[a]

protein	pressure at peak intensity [MPa]	$p_{1/2}$ [MPa]	quantum yield[24]	intensity gain I_{max}/I_0	variability $I_{max}/(I_0 \cdot p_{1/2})$ [GPa^{-1}]
mCherry	0	300	0.16	1	3.3
mKO	0	530	0.60[8]	1	1.9
TagRFP-S	250	500	0.48	1.25	2.5
TagRFP-T	280	700	0.47	2.5	3.6
mStrawberry	350	670	0.35	1.8	2.7
mOrange2	530	1130	0.55	1.25	1.1

[a]The pressure where the fluorescence intensity reaches half its maximum value is denoted $p_{1/2}$ and is a measure of stability against pressure effects. The column denoted I_{max}/I_0 shows the ratio of the fluorescence intensities at their maximum pressures and at ambient pressure. The value $I_{max}/(I_0 \cdot p_{1/2})$ can be used as a measure of variability.

dx.doi.org/10.1021/jp306093h | J. Phys. Chem. B 2012, 116, 10311−10316

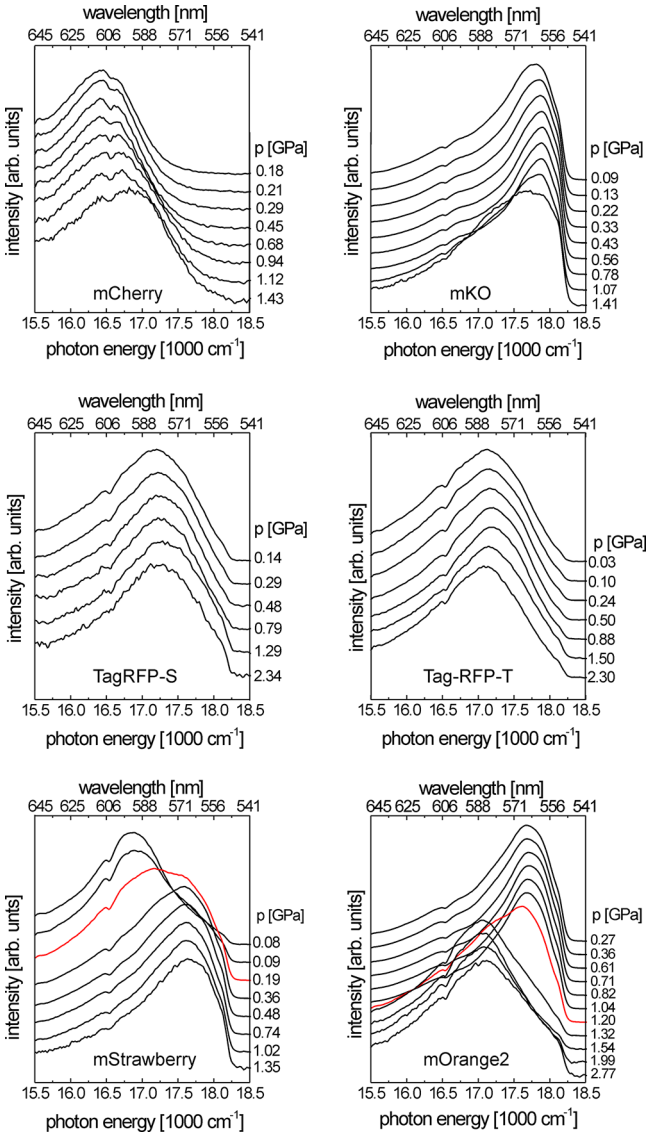

Figure 3. Pressure-dependent fluorescence intensity curves of mCherry (top left), mKO (top right), TagRFP-S (center left), TagRFP-T (center right), mStrawberry (bottom left) and mOrange2 (bottom right). The pressure for each spectrum is shown at the right side of the corresponding panel. The dip at 16.5 × 10^3 cm^{-1} in the spectra is an artifact of the spectrometer, the cutoff of the fluorescence spectra at ca. 18.5 × 10^3 cm^{-1} is due to the long-pass filter used to block the excitation laser radiation. All spectra have been normalized to have common peak intensities. The traces belonging to the pressures at which abrupt changes occur in the fluorescence spectra of mStrawberry and mOrange2 have been marked in red.

200 MPa. Interestingly, the change in the spectrum is concomitant with the fluorescence intensity increase observed in this RFP. The blue-shifted peak persists throughout the higher pressures, while the peak characteristic of the ambient pressure spectrum disappears. At the pressure where the fluorescence intensity reaches its maximum, the high-pressure spectrum is already fully developed and dominates the spectrum. In contrast, mOrange2 shifts its fluorescence spectrum abruptly by ca. 610 cm^{-1} to the red (from 566 to 587 nm) at around 1.2 GPa, where the fluorescence intensity reaches half its peak value. The signature of the chromophore at ambient pressures disappears, and the red-shifted peak persists at higher pressures.

The abrupt changes in the fluorescence spectra that are coupled to strong gains or losses in intensity suggest that these changes are caused by abrupt structural changes of the chromophore pocket, of the H-bonding configuration of the chromophore or even of the chromophore itself. *Cis*−*trans* isomerization has been implicated in similarly strong changes in the absorption spectrum of the RFP eqFP611.[34,35] A possible explanation of the behavior of mOrange2 involving covalent modification of the chromophore could involve a decyclization of the dihydrooxazole ring of the chromophore. Such a reaction could occur as a proton-catalyzed ring-opening, resulting in an increase in the conjugation length of the chromophore and the concomitant red shift. Hydrostatic pressure could be the driving force for this reaction and push the resulting modified chromophore into planarity. The magnitude of the red shift can be easily estimated, since it would result in a conjugated system similar to the chromophore of dsRed. The maximum of dsRed fluorescence at 583 nm is in close agreement with the maximum of the shifted fluorescence at 587 nm. Such a putative reaction would be the inverse of the maturation reaction as proposed by Kikuchi et al.[8]

The calculations on mStrawberry described by Laurent et al.[23] indicate the presence of two dominant conformations whose spectra and pressure trends agree very well with our experimental observations. There are two major structural differences between the two conformers. The hydrogen bonding environment of the chromophore's phenolate moiety changes, brought about by flipping the Ser146 residue. In addition, the distance of Lys70 to the phenolate-imidazolinone bridge changes significantly. We note that Lys70 is a conserved residue in all RFPs and its role in chromophore maturation has been recently demonstrated.[36] These changes lead to a stabilization of the S_0 ground state and result in a blue shift on the absorption spectrum which is in qualitative agreement with the experimentally observed blue shift in the fluorescence spectrum. Our observations are consistent with a change in the relative populations of the two calculated conformers.

■ CONCLUSIONS

We can clearly observe that proteins with very similar chromophores exhibit diverse behavior. The TagRFPs studied here differ only in residue 158, where a serine in the chromophore pocket has been exchanged for a threonine,[37] resulting in a pronounced change in pressure behavior. The variants mCherry and mStrawberry have identical chromophores, yet their response to high pressure is very different. Similarly, mKO and mOrange2 have nearly the same chromophores, but they also react very differently to pressure. These observations highlight that the properties of the barrel and of the pocket are more important for the pressure behavior of a FP than those of the chromophore itself.

The increase in fluorescence intensity observed for TagRFP-S, TagRFP-T, mOrange2 and mStrawberry are mostly due to an increase in quantum yield at intermediate pressures caused by a pressure induced increase in rigidity and stabilization of the chromophore. The observed drastic change in the fluorescence spectrum of mStrawberry at intermediate pressure can be traced to changes in the population of two conformers with different H-bonding environments of the chromophore (while retaining the overall conformation of the chromophore itself).[23]

dx.doi.org/10.1021/jp306093h | *J. Phys. Chem. B* 2012, 116, 10311−10316

With regard to future engineering of brighter RFPs, an increase in fluorescence intensity upon pressurization suggests that the fluorescence intensity at ambient pressure can be improved by variation of the protein barrel and/or the core residues to optimize geometry and rigidity of the chromophore and its environment. Optimization of a cyan FP along these lines has recently been reported.[29] However, it takes a detailed look at the pressure-induced changes to determine the precise changes to the protein that could lead to possible optimization of a particular FP through genetic engineering. Such information can be obtained either by simulations[23] or by high pressure experiments involving methods that are sensitive to structure, for example, anti-Stokes Raman studies.

AUTHOR INFORMATION

Corresponding Author

*E-mail: weberjm@jila.colorado.edu.

Notes

The authors declare no competing financial interest.

ACKNOWLEDGMENTS

J.M.W. gratefully acknowledges funding through the Innovative Grant Program of the University of Colorado at Boulder. This work was supported by NIH GM083849 (to R.J.). R.J. is a staff member in the Quantum Physics Division of NIST. We thank Prof. Prem Chapagain and Prof. Anna Krylov for sharing their data from molecular dynamics simulations of RFPs prior to publication. We also thank Kevin Dean and Professors Barney Ellison, David Nesbitt and Amy Palmer for helpful discussions and suggestions. We acknowledge Caitlin Majlinger for technical assistance.

REFERENCES

(1) Tsien, R. Y. *Annu. Rev. Biochem.* **1998**, *67*, 509−544.
(2) Day, R. N.; Davidson, M. W. *Chem. Soc. Rev.* **2009**, *38*, 2887−2921.
(3) Lin, M. Z.; McKeown, M. R.; Ng, H. L.; Aguilera, T. A.; Shaner, N. C.; Campbell, R. E.; Adams, S. R.; Gross, L. A.; Ma, W.; Alber, T.; Tsien, R. Y. *Chem. Biol.* **2009**, *16*, 1169−1179.
(4) Shu, X. K.; Shaner, N. C.; Yarbrough, C. A.; Tsien, R. Y.; Remington, S. J. *Biochemistry* **2006**, *45*, 9639−9647.
(5) Shaner, N. C.; Campbell, R. E.; Steinbach, P. A.; Giepmans, B. N. G.; Palmer, A. E.; Tsien, R. Y. *Nat. Biotechnol.* **2004**, *22*, 1567−1572.
(6) Henderson, J. N.; Remington, S. J. *Proc. Natl. Acad. Sci. U.S.A.* **2005**, *102*, 12712−12717.
(7) Remington, S. J.; Wachter, R. M.; Yarbrough, D. K.; Branchaud, B.; Anderson, D. C.; Kallio, K.; Lukyanov, K. A. *Biochem.* **2005**, *44*, 202−212.
(8) Kikuchi, A.; Fukumura, E.; Karasawa, S.; Mizuno, H.; Miyawaki, A.; Shiro, Y. *Biochem.* **2008**, *47*, 11573−11580.
(9) Remington, S. J. *Curr. Opin. Struct. Biol.* **2006**, *16*, 714−721.
(10) Subach, O. M.; Malashkevich, V. N.; Zencheck, W. D.; Morozova, K. S.; Piatkevich, K. D.; Almo, S. C.; Verkhusha, V. V. *Chem. Biol.* **2010**, *17*, 333−341.
(11) Scheyhing, C. H.; Meersman, F.; Ehrmann, M. A.; Heremans, K.; Vogel, R. F. *Biopolymers* **2002**, *65*, 244−253.
(12) Weber, G.; Drickamer, H. G. *Q. Rev. Biophys.* **1983**, *16*, 89−112.
(13) Choukroun, M.; Grasset, O. *J. Chem. Phys.* **2007**, *127*, No. 124506.
(14) Ehrmann, M. A.; Scheyhing, C. H.; Vogel, R. F. *Lett. Appl. Microbiol.* **2001**, *32*, 230−234.
(15) Leiderman, P.; Huppert, D.; Remington, S. J.; Tolbert, L. M.; Solntsev, K. M. *Chem. Phys. Lett.* **2008**, *455*, 303−306.
(16) Verkhusha, V. V.; Pozhitkov, A. E.; Smirnov, S. A.; Borst, J. W.; van Hoek, A.; Klyachko, N. L.; Levashov, A. V.; Visser, A. *Biochim. Biophys. Acta - Gen. Subj.* **2003**, *1622*, 192−195.
(17) Malavasi, N. V.; Foguel, D.; Bonafe, C. F. S.; Braga, C.; Chura-Chambi, R. M.; Vieira, J. M.; Morganti, L. *Process Biochem.* **2011**, *46*, 512−518.
(18) Mauring, K.; Krasnenko, V.; Miller, S. *J. Luminesc.* **2007**, *122*, 291−293.
(19) Mauring, K.; Deich, J.; Rosell, F. I.; McAnaney, T. B.; Moerner, W. E.; Boxer, S. G. *J. Phys. Chem. B* **2005**, *109*, 12976−12981.
(20) Herberhold, H.; Marchal, S.; Lange, R.; Scheyhing, C. H.; Vogel, R. F.; Winter, R. *J. Mol. Biol.* **2003**, *330*, 1153−1164.
(21) Barstow, B.; Ando, N.; Kim, C. U.; Gruner, S. M. *Proc. Natl. Acad. Sci. U.S.A.* **2008**, *105*, 13362−13366.
(22) Barstow, B.; Ando, N.; Kim, C. U.; Gruner, S. M. *Biophys. J.* **2009**, *97*, 1719−1727.
(23) Laurent, A. D.; Mironov, V. A.; Chapagain, P. P.; Nemukhin, A. V.; Krylov, A. I. *J. Phys. Chem. B* **2012**, submitted.
(24) Holzapfel, W. B. *J. Appl. Phys.* **2003**, *93*, 1813−1818.
(25) Deich, J. A.; Mauring, K.; Rosell, F. I.; McAnaney, T. B.; Moerner, W. E.; Boxer, S. G. *Biophys. J.* **2002**, *82*, 427A.
(26) Krasnenko, V.; Tkaczyk, A. H.; Tkaczyk, E. R.; Mauring, K. *Biopolymers* **2008**, *89*, 1136−1143.
(27) Gekko, K.; Hasegawa, Y. *Biochem.* **1986**, *25*, 6563−6571.
(28) Kharakoz, D. P. *Biophys. J.* **2000**, *79*, 511−525.
(29) Goedhart, J.; von Stetten, D.; Noirclerc-Savoye, M.; Lelimousin, M.; Joosen, L.; Hink, M. A.; van Weeren, L.; Gadella, T. W. J.; Royant, A. *Nat. Commun.* **2012**, *3*, No. 751.
(30) Dean, K. M.; Lubbeck, J. L.; Binder, J. K.; Schwall, L. R.; Jimenez, R.; Palmer, A. E. *Biophys. J.* **2011**, *101*, 961−969.
(31) Donnert, G.; Eggeling, C.; Hell, S. W. *Nat. Methods* **2007**, *4*, 81−86.
(32) Royer, C. A. *Braz. J. Med. Biol. Res.* **2005**, *38*, 1167−1173.
(33) Hummer, G.; Garde, S.; Garcia, A. E.; Paulaitis, M. E.; Pratt, L. R. *Proc. Natl. Acad. Sci. U.S.A.* **1998**, *95*, 1552−1555.
(34) Yan, W. Z.; Xie, D. Q.; Zeng, J. *Phys. Chem. Chem. Phys.* **2009**, *11*, 6042−6050.
(35) Loos, D. C.; Habuchi, S.; Flors, C.; Hotta, J. I.; Wiedenmann, J. R.; Nienhaus, G. U.; Hofkens, J. *J. Am. Chem. Soc.* **2006**, *128*, 6270−6271.
(36) Bravaya, K. B.; Subach, O. M.; Korovina, N.; Verkhusha, V. V.; Krylov, A. I. *J. Am. Chem. Soc.* **2012**, *134*, 2807−2814.
(37) Shaner, N. C.; Lin, M. Z.; McKeown, M. R.; Steinbach, P. A.; Hazelwood, K. L.; Davidson, M. W.; Tsien, R. Y. *Nat. Methods* **2008**, *5*, 545−551.